Mass Property Estimation for Control of Asymmetrical Satellites

E. V. Bergmann*
The Charles Stark Draper Laboratory, Inc., Cambridge, Massachusetts

B. K. Walker†
University of Cincinnati, Cincinnati, Ohio

D. R. Levy‡
U.S. Air Force Space Division, Los Angeles, California

Real-time algorithms that estimate the mass-property parameters commonly used in spacecraft control laws are developed based upon a stochastic estimation viewpoint. The elements of the inverse inertia matrix and the center-of-mass location vector are estimated from noisy measurements of the angular velocity using a second-order filter, while estimates of the mass reciprocal are generated from noisy linear velocity measurements using a Kalman filter. Simulation results show that the rate of convergence of each estimate depends strongly upon the particular maneuver being performed, but that the mass properties can be estimated to within 1% error.

Introduction

As space systems become larger and more complex, the demands for controlling these systems correspondingly increase. For the case of stationkeeping and attitude control, it becomes desirable to implement control algorithms that can automatically adapt themselves as the spacecraft configuration changes. Such changes might be the result of releasing a payload from a shuttle orbiter, a satellite retrieval, one spacecraft docking with another, or a construction phase where one section of a satellite or station remains operational while other modules are being attached. Another possibility is that the configuration might not be known very well (e.g., grapple of debris or asteroid), or it might be changing in an unpredictable way (e.g., sloshing fuel, crew movement, extending appendages).

In each of these cases, reliable and efficient attitude control requires accurate knowledge of the changing vehicle mass properties. This paper presents a method of recursively estimating and tracking the mass properties given noisy measurements of the translational and angular velocities of the vehicle and knowledge of the control inputs.

The methods developed here produce estimates of the mass properties needed by a wide variety of attitude control algorithms. However, the emphasis here is on the advanced autopilot recently flight tested on the space shuttle orbiter.[1] Control of the shuttle is provided by a redundant, nonsymmetric set of reaction control jets. These jets are commanded to fire by the jet selection in combinations such that desired changes in the translational velocities and angular velocities will be achieved. This jet selection problem is formulated as a linear programming problem as follows.

Let each jet be characterized by an activity vector comprising the expected angular and linear accelerations resulting from the firing of that jet, i.e. for the jth jet

$$a_j = \begin{bmatrix} I^{-1}(r_j - r_{cm}) \times T_j \\ \hline m^{-1} T_j \end{bmatrix} \tag{1}$$

where I is the vehicle inertia matrix, r_j is the position of the jth jet with respect to the vehicle reference frame, r_{cm} is the position of the vehicle center of mass relative to the vehicle reference frame, T_j is the (known) thrust of the jth jet, expressed in vehicle coordinates, and m is the vehicle mass. Notice that a_j is strongly dependent upon the mass properties, I^{-1}, r_{CM} and m^{-1}. The requested rate changes can be expressed as a linear combination of the activity vectors

$$\begin{bmatrix} \Delta w \\ \hline \Delta v \end{bmatrix} = \sum_{j=1}^{n} a_j t_j \tag{2}$$

where n is the number of jets, t_j is the firing time for the jth jet, and Δw and Δv are the requested angular and linear rate changes, respectively. Physically realizable solutions add a constraint:

$$t_j \geq 0 \qquad j = 1,2,\ldots,n \tag{3}$$

The problem is thus to choose those jets and their firing times that satisfy Eqs. (2) and (3) (provided such a set exists) and simultaneously minimize a linear cost function based on fuel usage which is proportional to the firing times of all the jets. The solution to this linear programming problem can be found by the simplex algorithm.[1,2]

In light of the dependence of a_j on I^{-1} (the inverse inertia matrix), r_{CM} (the center of mass position) and m^{-1} (the reciprocal mass), these are the quantities to be estimated. The estimation algorithm must be sufficiently simple that it can be implemented on-line in real time. It must also be capable of reliably and quickly tracking changes in the mass properties

Presented as Paper 85-1857 at the AIAA Guidance, Navigation, and Control Conference, Snowmass, CO, Aug. 19-21, 1985; received Oct. 1985; revision received July 1986.

*Section Chief, Control and Flight Dynamics Divison. Member AIAA.

†Associate Professor of Aerospace Engineering and Engineering Mechanics. Senior Member AIAA.

‡Captain, U.S. Air Force. Member AIAA.

without being overly sensitive to sensor noise. Such a problem suggests an optimization approach, provided we can model the sensor noise correctly. The estimator should also be relatively insensitive to slight uncertainties in "known" parameters such as the commanded vehicle thrusts. However, there is usually a trade-off between the degree of robustness in an algorithm and that algorithm's performance when the model is known exactly.[3] For this reason—as well as the desire to keep the jet selection informed—we shall not require that the mass property estimator be insensitive to large parameter deviations that are the result of jet failures. Rather, any jet failures shall be detected and isolated by a separate procedure, which in turn must be intelligent enough not to be confused by large jumps in the mass properties.

The rotational dynamics of a rigid body can be described in terms of the applied forces by

$$I\Delta\omega = \sum_i \boldsymbol{r}_i \times \boldsymbol{F}_i \Delta t + \boldsymbol{M}_d \Delta t \tag{4}$$

where

Δt = time step
I = vehicle inertia matrix
$\Delta\omega$ = change in angular rate
$\boldsymbol{r}_i$ = lever arm of force i
$\boldsymbol{F}_i$ = force i
$\boldsymbol{M}_d$ = the sum of all disturbance torques

We shall assume that the angular rates are small, so that during periods of jet activity the dynamic coupling effects over the sample interval can be treated as small disturbance torques. If we have confidence in the estimates of I and the measurements of ω, this disturbance torque can be treated as a known disturbance torque and accurately estimated. Otherwise, it must be treated as an unmodeled noise. Such an approach will usually be reasonable because the "signal" torque due to the jet moments will typically be several orders of magnitude greater than the cross-coupling "noise" torque.

Throughout its mission, a spacecraft will also be affected by a number of other disturbance forces and torques such as aerodynamic drag and gravity gradients, some of which may disturb the vehicle even more than the cross coupling. As with the dynamic coupling, these disturbances may or may not be accurately estimated from a priori knowledge and sensor information. In the majority of cases, however, these disturbances will be small and may not even be measurable; consequently, we shall treat them, like the dynamic coupling torques, as noises.

By including the known disturbance forces and torques in our model and assuming no jet failures, Eq. (4) becomes

$$I\Delta\omega = \sum_i \boldsymbol{r}_i \times \boldsymbol{T}_i \Delta t + \sum_i \boldsymbol{r}_{d_i} \times \hat{\boldsymbol{E}}_{d_i} + \hat{\boldsymbol{M}}_d \Delta t \tag{5}$$

Here, $\boldsymbol{T}_i$ is the known applied thrust of the ith firing jet, located by the vector $\boldsymbol{r}_i$ from the center of mass; $\hat{\boldsymbol{E}}_{d_i}$ is the ith known disturbance force, located at $\boldsymbol{r}_{d_i}$ relative to the center of mass; and $\hat{\boldsymbol{M}}_d$ is the resultant of all known disturbance torques not due to $\hat{\boldsymbol{E}}_{d_i}$.

Now define the state vector $\boldsymbol{x}$ consisting of the nine mass property parameters in Eq. (5) that we want to estimate

$$\boldsymbol{x}^{\Delta} = [I_{11}^{-1},\ I_{22}^{-1},\ I_{33}^{-1},\ I_{23}^{-1}, I_{13}^{-1},\ I_{12}^{-1},\ r_{cm_1},\ r_{cm_2},\ r_{cm_3},]^T \tag{6}$$

where I_{ij}^{-1} is the element in the ith row and jth column of the inverse inertia matrix and r_{cm_i} is the ith element of r_{cm}. Notice that the mass m does not appear in Eq. (5) and hence not in Eq. (6). Estimation of m^{-1} will be considered separately later in this paper.

Let:

$$\lambda = \sum_i \boldsymbol{T}_i \Delta t + \sum_i \hat{\boldsymbol{E}}_{d_i} \Delta t \tag{7a}$$

and

$$\alpha = \sum_i \boldsymbol{r}_i \times \boldsymbol{T}_i \Delta t + \sum_i \boldsymbol{r}_{d_i} \times \hat{\boldsymbol{E}}_{d_i} \Delta t + \hat{\boldsymbol{M}}_d \Delta t \tag{7b}$$

Then a measurement can be formulated in terms of the state:

$$\boldsymbol{h}(\boldsymbol{x}) = A\boldsymbol{x} + \frac{1}{2}\sum_{i=1}^{3} \boldsymbol{\phi}_i \boldsymbol{x}^T \Lambda^i \boldsymbol{x} \tag{7c}$$

where ϕ_i, ϕ_2, and ϕ_3 are the natural basis vectors in R^3. The matrices A, Λ_1, Λ_2, and Λ_3 are given in Ref. 7. A is a 3×9 matrix with zeroes in its last 3 columns and the elements of α, the angular velocity impulses due to the applied forces and torques, appearing elsewhere. Each Λ_i is a 9×9 symmetric matrix with an upper left 6×6 partition and a lower right 3×3 partition comprised entirely of zeroes. The remaining elements are zero or elements of λ, the linear velocity impulses due to the applied forces and torques.

Note that by neglecting the second-order terms, one obtains the simple linear measurement equation:

$$\boldsymbol{h}(\boldsymbol{x}) = A\boldsymbol{x}$$

However, because the last 3 columns of A consist entirely of zeroes, λ_{CM} does not appear in this linear measurement equation. Therefore, we must use the complete nonlinear model [Eq. (7)] if we want to estimate r_{cm}. Furthermore, we discover that the center-of-mass position cannot be uniquely determined when there is no net translational force.

The measurement equation (7) assumes that measurements of the angular rate are available, which is clearly the case when rate gyroscopes are in operation. If, instead, the attitude of the spacecraft is available, as would be the case with integrating gyros, horizon, sun, star, magnetic gradient, or gravity-gradient sensors, then the available measurements must be differentiated to find the angular rate. Often, a full state observer for the attitude and its first two derivatives is used, in which case the appropriate parameters can be picked out. However, the bandwidth of such observers must be carefully examined because severely bandwidth-limited measurements will undoubtedly degrade the performance of any real-time algorithms based on them.[4]

The discrete angular velocity change measurement at each time instant is assumed to satisfy the stochastic equation

$$z_k = \omega_k + v_k^{\omega} - v^{\omega}{}_{k-1} \tag{8}$$

where z_k is the indicated change from the sensor package, ω_k is the true value of the angular velocity at time k, and v_k^{ω} is a three-dimensional white Gaussian sequence independent of $\boldsymbol{x}_k$ and all forces and torques, with zero mean and covariance R_k^{ω}. The measurement equation becomes

$$z_k = \boldsymbol{h}(\boldsymbol{x}_k) + v_k^z \tag{9}$$

State Dynamics

In the simplest case, the deterministic model for the state dynamics can be described in discrete time as

$$\boldsymbol{x}_{k+1} = \boldsymbol{x}_k \tag{10}$$

It is desirable, however, to include process "noise" in the model in order to prevent the filter from becoming overly optimistic after a long period of time. Should it become too optimistic, the filter will ignore good recent data and thus fail to properly track slow variations in $\boldsymbol{x}$ as they occur. Additionally,

the state may actually vary in some unmodeled (although perhaps not random) manner due to fuel expenditure, astronaut movements, vibrating appendages, etc. Therefore, we choose a discrete stochastic model for the state dynamics that includes a single step transition matrix other than identity (call it ϕ) and fictitious noise whose statistics are based on the magnitude of the expected state variations during each sample period. These statistics can also be varied in order to "tune" the filter to achieve particular response properties.

With an additive noise term, Eq. (10) takes the general form

$$x_{k+1} = \phi x_k + \Gamma w_k \tag{11}$$

where $\{w_k\}$ is the hypothesized nine-dimensional white Gaussian sequence independent of x_k with

$$E[w_k] = 0 \tag{12}$$

$$E[w_k w_k^T] = Q_k \geq 0 \tag{13}$$

and Γ is simply introduced for generality.

Finally, if unknown jumps in the mass properties occur at infrequent periods of time, perhaps due to docking maneuvers or satellite deployments, then Eq. (11) can be modified with an additional term

$$x_{k+1} = \phi x_k + \Gamma w_k + \delta_{k+1;\theta} \nu \tag{14}$$

where ν is the value of the unknown jump, θ is the time interval in which the jump occurs, and $\delta_{k;\theta}$ is the Kroenecker delta, defined as

$$\delta_{k;\theta} \triangleq \begin{cases} 1 \text{ if } k = \theta \\ 0 \text{ otherwise} \end{cases} \tag{15}$$

Discussion of how to deal with such jumps appears in a later section.

Nonlinear (Second-Order) Filter

Let $\hat{x}_{k/j}$ represent the estimate of x at time step k given measurements z_k up to and including time step j. Let $S_{k/j}$ be the computed error covariance of this estimate. A second order filter, such as that of Ref. 3 (Sec. 6.1) or the truncated second order filter of Ref. 8 (Sec. 9.3) produces the following linear measurement update equation:

$$\hat{x}_{k/k} = \hat{x}_{k/k-1} + K_k e_k \tag{16}$$

$$S_{k/k} = S_{k/k-1} - K_k H_k(\hat{x}_{k/k-1}) S_{k/k-1} \tag{17}$$

where the measurement residual is

$$e_k = z_k - h_k(\hat{x}_k) \tag{18}$$

and where the second order measurement equation is

$$h_k(\hat{x}_k) = h_k(\hat{x}_{k/k-1}) + \frac{1}{2}\sum_{i=1}^{3} \phi_i \text{tr}(\tilde{H}_k^i S_{k/k-1}) \tag{19}$$

The filter gain is

$$K_k = S_{k/k-1} H_k^T(\hat{x}_{k/k-1}) Y_k^{-1} \tag{20}$$

where

$$Y_k = H_k(\hat{x}_{k/k-1}) S_{k/k-1} H_k^T(\hat{x}_{k/k-1}) + D_k + R_k^z \tag{21}$$

$$D_k = \frac{1}{2}\sum_{i=1}^{3}\sum_{j=1}^{3} \phi_i \phi_j^T \text{tr}(\tilde{H}_k^i S_{k/k-1} \tilde{H}_k^j S_{k/k-1}) \tag{22}$$

$$H_k^i(\hat{x}_{k/k-1}) = A_k^i + \hat{x}_{k/k-1}^T \Lambda_k^i \tag{23}$$

$$\tilde{H}_k^i(\hat{x}_{k/k-1}) = \Lambda_k^i \tag{24}$$

where $H_k^i(\hat{x}_{k/k-1})$ and A_k^i denote the ith rows of $H_k(\hat{x}_{k/k-1})$ and A_k, respectively. Note that the Hessian is independent of the state estimate [i.e., $\tilde{H}^i(\hat{x}_{k/k-1}) = \tilde{H}_k^i$].

Between measurements, the estimate and error covariance are updated according to

$$\hat{x}_{k+1/k} = \phi \hat{x}_{k/k} \tag{25}$$

$$S_{k+1/k} = \phi S_{k/k} \phi^T + \Gamma Q_{k+1} \Gamma^T \tag{26}$$

Alternate Form

The second-order filter Eqs. (16)–(24) closely resembles the extended Kalman filter. The differences are an additional bias term in Eq. (19) and the D_k matrix in Eq. (21). These corrections represent the effect of the Hessian matrices that the extended Kalman filter does not consider. In fact, if one sets the Hessian matrices to zero, one obtains the extended Kalman filter equations exactly.

The importance of the nonlinearity in the estimation scheme is evident when examining Eqs. (19) and (21). In the latter, the nonlinearity appears as a "noise" that is added to the measurement noise. When the measurement noise is large compared to the second-order term, the nonlinearity is masked by the measurement noise. When the opposite is true, however, the nonlinearity is significant and neglecting this term will yield poor estimation performance. In terms of the filter parameters, Eq. (21) indicates that the nonlinearities are significant when

$$D_k \gtrsim R_k^z \tag{27}$$

During the initial periods of estimation, when S, and thus D, are relatively large, we must take care to use the complete second-order filter. Once the filter has approached its steady-state (if any) and S has become very small, however, the nonlinearities become negligible relative to the measurement noise and little is gained by using a second-order filter as opposed to the extended Kalman filter. (For a further examination of this phenomenon, see Ref. 5.)

For this particular system, the Hessian matrices are sparse. By accounting for this fact during implementation, the amount of additional computations required by the second-order filter relative to the extended Kalman filter will not be significant.

Lastly, we note that since the Jacobian matrix depends upon the states, and both the Jacobian and Hessian matrices depend upon the time-varying applied forces, the propagation of the error covariances cannot be precomputed. Therefore, the gains must be computed in real time, and in fact the concept of a steady-state gain has no meaning for this problem.

Adaptive Filtering by Covariance Incrementation.

We have shown that the state dynamics in the presence of an occasional large jump in the state can be modeled by the stochastic difference equation for the state

$$x_k = \phi x_{k-1} + \Gamma w_k + \delta_{k,\theta} \nu \tag{28}$$

However, if there is only a small number of known applied impulse configurations, such that one always uses an element from a known finite set of combinations and *if* the state to be estimated is time-invariant, then there may be a set of steady-state gains—one for each impulse configuration. Unfortunately, these gains will also depend upon the value of the steady-state estimate, which is unknown at the beginning of the problem.

We wish to design a method whereby the filter equations developed in the last section can be adapted automatically to incorporate the jump in the state estimate. One typical ap-

proach to this problem involves estimating θ and ν from the residual history and then using these estimates in a decision rule that decides whether a jump has occurred. If the decision is then made that a jump has in fact occurred, the estimates $\hat{\theta}$ and $\hat{\nu}$ are used to correct the state estimate $\hat{x}$ accordingly. Such an approach is known as the generalized likelihood ratio (GLR) technique, and the estimates $\hat{\theta}$ and $\hat{\nu}$ so generated are the maximum likelihood estimates [6]. Unfortunately, the nonlinearity of the measurement function and the dependence of the filter gains on the state estimates prevent this approach from working. Therefore, a modified approach that does not require estimates of ν and θ has been pursued here.

Consider the two hypotheses:

H_0: No jump to the present time ($\theta > k$)
H_1: A jump has occurred ($\theta < k$)

Our approach is to devise a test that will decide between H_0 and H_1 based on a consistency check. If the residuals are not consistent with their statistics (and if no jet failures have yet been indicated), then H_1 is decided and the estimation error covariance matrix S in the second-order filter is increased. The rationale behind this approach is based on the fact that after a jump much larger than the process noise has occurred, the filter becomes optimistic and thus does not sufficiently weight the new measurements. By increasing the diagonal elements of the noise covariance matrix Q_k (which are set to the squared values of the components of a typical jump) during the interval of detection, the error covariance matrix becomes large and this problem is corrected.

By assuming that $\theta = k$ under H_1, the two hypotheses can be written in terms of the residual as

$$H_0: e_k = e_k^0 \quad (\theta > k) \tag{29}$$

$$H_1: e_k = e_k^0 + \mu_k(\nu) + N_k(\nu)\hat{x}_{k/k-1}^0 \quad (\theta = k) \tag{30}$$

where the superscript 0 denotes the part of the applicable vector that is generated by all effects *except* those due to the jump. We know that e_k^0 and $\hat{x}_{k/k-1}^0$ are zero mean random rectors with covariances Y_k and $S_{k/k-1}$, respectively. To determine $\mu_k(\nu)$ and $N_k(\nu)$, note that:

$$\begin{aligned} e_k &= h_k(x_k) + v_k^z - \hat{h}_k(x_k) \\ &= A_k(x_k^0 + \nu) + \frac{1}{2}\sum_{i=1}^{3}\phi_i(x_k^0+\nu)^T\Lambda_k^i(x_k^0+\nu)] + v_k^z - \hat{h}_k(x_k) \\ &= e_k^0 + h_k(\nu) + \sum_{i=1}^{3}\phi_i\nu^T\Lambda_k^i\hat{x}_{k/k-1}^0 + \sum_{i=1}^{3}\phi_i\nu^T\Lambda_k^i\hat{x}_{k/k-1}^0 \end{aligned} \tag{31}$$

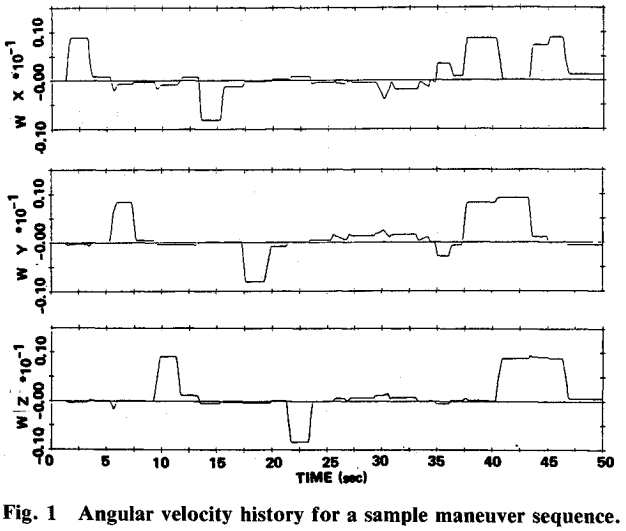

Fig. 1 Angular velocity history for a sample maneuver sequence.

Therefore

$$N_k(\nu) = \sum_{i=1}^{3}\phi_i\nu^T\Lambda_k^i \tag{32}$$

and

$$\mu_k(\nu) = h_k(\nu) + \sum_{i=1}^{3}\phi_i\nu^T\Lambda_k^i\hat{x}_{k/k-1}^0 = h_k(\nu) + N_k(\nu)\hat{x}_{k/k-1}^0 \tag{33}$$

Under H_1, the mean and covariance of the residual are

$$E\{e_k|H_1\} = \mu_k(\nu) \tag{34}$$

$$\begin{aligned} &E\{[e_k - \mu_k(\nu)][e_k - \mu_k(\nu)]^T|H_1\} \\ &= Y_k + N_k(\nu)S_{k/k-1}H_k^T(\hat{x}_{k/k-1}^0) \\ &+ H_k(\hat{x}_{k/k-1}^0)S_{k/k-1}N_k^T(\nu) + N_k(\nu)S_{k/k-1}N_k^T(\nu) \\ &\triangleq M_k(\nu) \end{aligned} \tag{35}$$

Now that the statistics of the residual are known under both hypotheses, we can use the decision rule

$$\text{decide } H_1, \text{ true if } L_k < \eta H_0 \text{ true if } L_k > \eta \tag{36}$$

where L_k is the single-sample generalized likelihood ratio defined

$$L_k \triangleq \frac{p(e_k|H_1, \theta = k,\ \mu_k = \hat{\mu}_k, M_k = \hat{M}_k)}{p(e_k|H_0)} \tag{37}$$

and η is some threshold.

Note that we defined the likelihood ratio in terms of μ_k and M_k rather than ν. This is done because we cannot estimate ν from only one residual, and if we use more than one residual, the estimation procedure becomes unbearably nonlinear. The estimate $\hat{\mu}_k$ is taken to be the maximum likelihood estimate

$$\hat{\mu}_k = \arg\max p(e_k|H_1, \mu_k = \tilde{\mu}_k) = e_k \tag{38}$$

and we shall let $\hat{M}_k$ be unspecified for the moment. Taking the logarithm of Eqs. (35) and (36) yields the test

$$\ell \triangleq 2lnL_k = e_k^T Y_e^{-1} e_n + ln\frac{|Y_k|}{|\hat{M}_k|} \underset{H_0}{\overset{H_1}{\gtrless}} 2ln\eta \tag{39}$$

Unfortunately, this test requires the maximum likelihood estimate of M_k, which cannot be determined from only one residual. However, (35) suggests that $|M_k| > |Y_k|$, in which case neglecting the applicable term in (38) gives a slightly lower (conservative) threshold. Our decision rule is then

$$\ell_k \approx e_k^T Y_k^{-1} e_k \underset{H_0}{\overset{H_1}{\gtrless}} \eta' \triangleq 2ln\eta \tag{40}$$

Instead of requiring that η be specified and that $|M_k| > |Y_k|$, the test threshold of η can also be selected directly by a Neyman-Pearson approach according to the known distribution of ℓ_k under H_0. When no jumps have occurred, the test statistic is a central χ^2 random variable with 3 degrees of freedom. By integrating the density function from $\ell = \eta'$ to $\ell = +\infty$ (or using a table), we can choose the threshold to yield a desired probability of false alarm (P_{FA}). For example, a threshold value of $\eta' = 11.34$ gives a P_{FA} of 1%, while the mean of the test statistic is 3. Alternately, the threshold can be based on the probability of detection (P_D) for a specified ν under H_1. Here, $e_k Y^{T-1} e_k$ becomes noncentrally χ^2 distributed with noncentrality parameter $\delta^2 = \mu_k(\nu)^T Y_k \mu_k(\nu)$ (provided that $|M_k| \approx |Y_k|$). Its mean is $3 + \mu_k(\nu) Y_k \mu_k(\nu)$. Of course, integrated noncentral χ^2 distributions are not generally available in tabulated form in the literature. (An algorithm that accomplishes such integrations is provided in Ref. 6.)

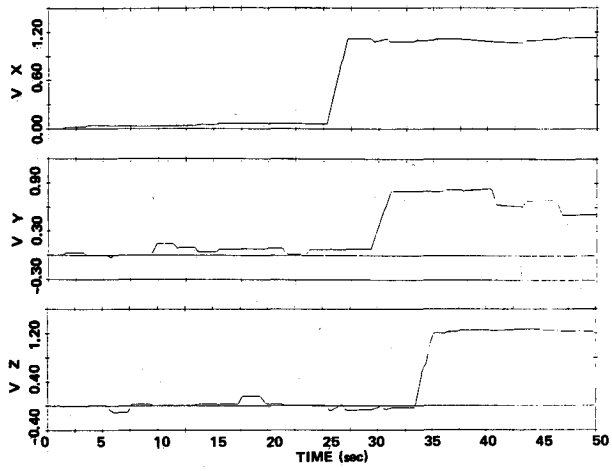

Fig. 2 Linear velocity hisory for a sample maneuver sequence.

In summary, we use the likelihood ratio test Eq. (40) to test our residuals for consistency. If the residuals are larger than expected and no jet failures are indicated, H_1 is decided and the process noise covariance matrix Q_k is increased over one sample period. The filter is then no longer optimistic and the jump in the state is tracked accordingly by the filter estimate.

Mass Estimation

The shuttle has redundant integrating accelerometers, each located by the vector r_j from the center of mass. The impulsive velocity change sensed by the jth accelerometer is governed by

$$\Delta V_j = m^{-1}\sum_i T_i \Delta t + \Delta\omega \times r_j + m^{-1}\sum_i \hat{E}_i^d \Delta t + m^{-1} E_j^d \Delta t \qquad (41)$$

where T_i is the thrust of the ith firing jet, $\hat{E}_i^d$ is the ith known external disturbance force, and E_j^d is the resultant of all unknown disturbance forces that affect the accelerometer (for a simple model, $E_i^d = 0$) where subscript j is used to signify the dependence of the subscripted quantity on the position of the sensor; e.g., certain gravity-gradient effects and the centripetal force are position dependent.

Now let λ be the linear momentum impulse caused by all the known forces given by Eq. (7a). Two types of rotational coupling must be considered. They are transverse acceleration τ_j and centripetal acceleration c_j. Including these, the measurement function then becomes

$$\Delta V_j = \lambda m^{-1} + \tau_j + c_j + v_j^d \qquad (42)$$

where v_j^d now represents the translational velocity disturbance due to external forces. It is assumed to be zero mean Gaussian with covariance R_k^d.

The estimation of m^{-1} based on the dynamics model and the measurement model is rather straight-forward if one assumes that the rotational coupling terms can be neglected. In this case, one simply implements a Kalman filter to obtain the optimum state estimate, because the applicable equations are linear. Because this approach is so simple, we shall handle the rotational coupling terms by estimating them and treating their estimation errors as additive noises. The estimated rotational terms are subtracted from the measurements to obtain a linear measurement ζ which is corrupted by zero-mean noise. Provided that the error covariance of this noise is known, we can then apply a Kalman filter.

Let $\hat{m}_{k/\ell}^{-1}$ and $\sigma_{k/\ell}^2$ denote the estimated reciprocal mass and its error variance, respectively, at the kth time instant based on ℓ measurements. Also, assume that $\hat{m}_{0/0}^{-1}$ and $\sigma_{0/0}^2$ are given. Then, the Kalman filter evolution between measurements for a constant scalar state is

$$\hat{m}_{k/k-1}^{-1} = m_{k-1/k-1}^{-1} \qquad (43)$$

$$\sigma_{k/k-1}^2 = \sigma_{k/k-1}^2 + q_k \qquad (44)$$

where q_k is a fictitious process noise variance added to prevent the filter from becoming too optimistic. The update across measurements is

$$\hat{m}_{k/k}^{-1} = m_{k/k-1}^{-1} + K_k \cdot \epsilon_k \qquad (45)$$

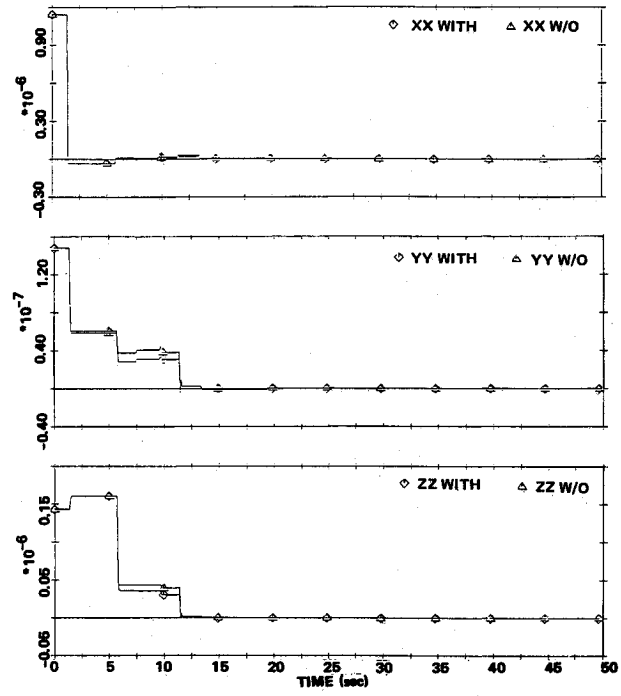

Fig. 3a Effect of dynamic coupling on inverse inertia estimates—diagonal elements.

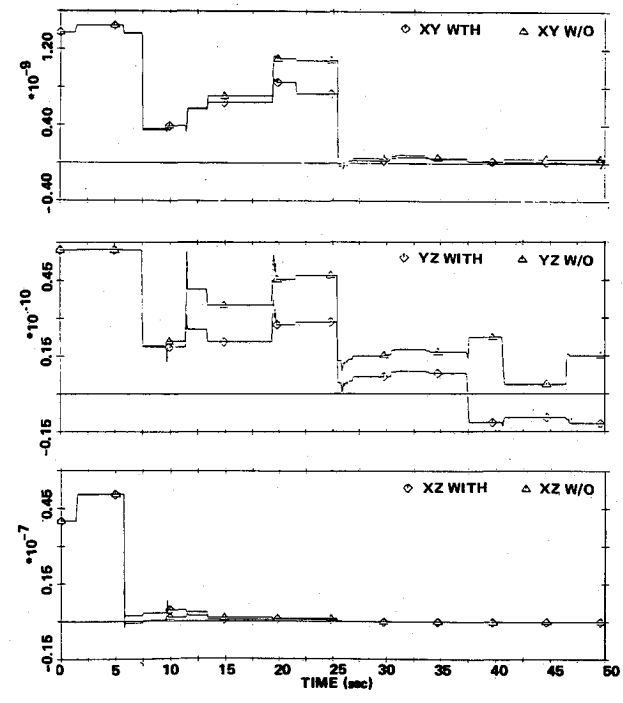

Fig. 3b Effect of dynamic coupling on inverse inertia estimates—off-diagonal elements.

$$\sigma^2_{k/k} = (1 - \boldsymbol{K}_k \cdot \boldsymbol{\lambda}_k)^2 \sigma^2_{k/k-1} + K_k^T R_k K_k \tag{46}$$

where

$$\epsilon_k = \Delta V_k - \boldsymbol{\lambda}_k \hat{m}^{-1}_{k/k-1} \tag{47}$$

$$\boldsymbol{K}_k^T = \sigma^2_{k/k-1} \boldsymbol{\lambda}_k^T Y_k^{-1} \tag{48}$$

$$Y_k = \sigma^2_{k/k-1} \boldsymbol{\lambda}_k \boldsymbol{\lambda}_k^T + R_k^{\zeta} \tag{49}$$

The measurement noise variance R_k^{ζ} is the covariance of the measurement ζ_k that has been corrected for the rotational coupling terms in Eq. (42).

The vector ϵ_k is the zero-mean residual that is fed back to correct the state. Its covariance is Y_k. Because this residual is well-characterized during normal operation, it can be monitored to detect special events such as mass-property jumps and jet-failures.

The Kalman gain vector $\boldsymbol{K}_k$ given by Eq. (48) is independent of the state but does depend upon the applied impulses $\boldsymbol{\lambda}_k$. Therefore, $\boldsymbol{K}_k$ will be time-varying, even if R_k^{ζ} and q_k are constant and $\sigma^2_{k/k-1}$ reaches a steady-state value. Thus, there will not be a single steady-state gain that can be precomputed to reduce the computations. It is conceivable, however, to use a set of steady state gains if $\boldsymbol{\lambda}_k$ is known to take on only a finite number of possible values (e.g., jet-firing combinations). Thus, it could be feasible to use a table of these gains when the number of possibilities is small, thereby saving a considerable amount of computation at the expense of some loss in performance. Of course, simulations should be done beforehand to verify that such an approach is acceptable.

Tests of the Algorithm

For the simulation runs described in this report, the autopilot was operated in the manual mode using the discrete-rate submode. A preset angular rate of 0.5 deg/s was commanded about a particular axis whenever the rotational hand controller (RHC) was out of detent in that axis; otherwise, the vehicle maintained an inertial attitude hold. For translation, a nearly constant linear acceleration (of about 0.5 ft/s^2) was commanded along a particular axis when the translational hand controller (THC) was out of detent in that axis; upon return to detent, the translation acceleration is zeroed.

Figures 1 and 2 illustrate the angular and linear velocities, respectively, for one typical set of vehicle maneuvers. (The linear velocity is taken relative to the initial velocity.) At 1 second the RHC is moved positively out of detent for the x-axis, and it is returned to detent at 3 s. From 5 to 7 s a similar action is taken for the Y-axis, and from 9 to 11 s a Z-axis rotation is accomplished. This entire maneuver sequence is then repeated for the negative rotations between 13 and 23 s. At 25 s the THC is positively positioned out of detent in the X-axis, where it remains until 27 s. The THC is next moved positively out of of detent in the Y-axis from 29 to 31 s, and in the Z-axis from 33 to 35 s. Finally, a set of three-second mixed rotational maneuvers are begun at 37 s. The RHC begins positively out of detent in the X- and Y-axes, but at 40 s the X-axis is returned while the Z-axis is positively activated. At 43 s the Y-axis is returned while the X-axis is positively set again, and at 46 s all controllers are returned while the X-axis is positively set again, and at 46 s all controllers are returned to detent.

These are merely selected as a representative set of maneuvers which excite motion about all body axes and should make all states observable. A strategy to minimize the jet firings and accelerate the convergence of the estimates is described in Ref. 9.

Note from Figs. 1 and 2 that there is some residual rotation during the translational maneuvers, while conversely there is some net translation during rotations. Additionally, there is some residual rotation about the other axes when a rotation is commanded about one particular axis. All this coupling occurs mainly because the jet configurations and inertia properties are not symmetric nor aligned with the vehicle axes. (There is also some small dynamic coupling.) Such coupled forces and torques actually enable us to observe some of the mass properties that would ordinarily be unobservable under a pure rotation or translation.

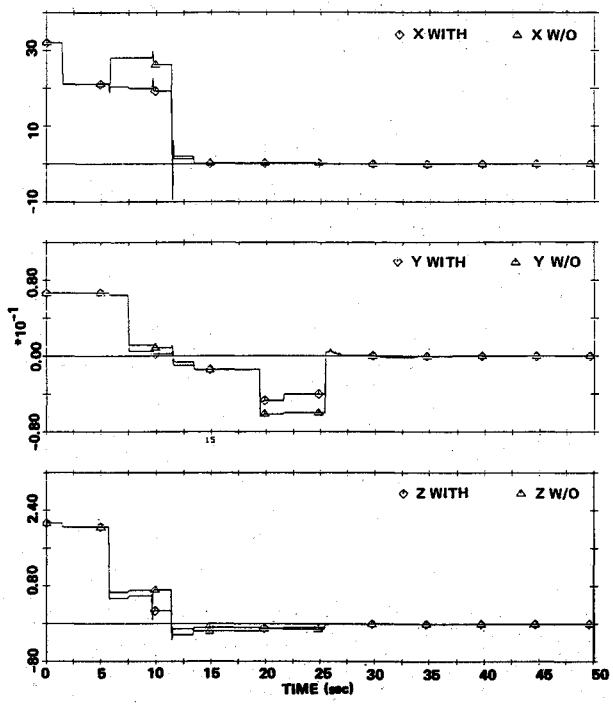

Fig. 4 Effect of dynamic coupling on center-of-mass location estimates—diagonal elements.

For the sample maneuver sequence just discussed, a total of 118 jet firings were commanded by the autopilot. Typical firings lasted from 80 ms to 640 ms for rotational requests, while some jets were on as long as the THC was out of detent (2 s) for translations. Since the mass-property estimates can be updated only when a known force or torque is applied (i.e., when at least one jet is commanded on), much of the simulation time took place when the mass properties were observable.

In order to eliminate the transient build-up of forces and torques generated when a jet is first commanded on or off, measurement data was only incorporated after the jet-firing combination had remained constant for one sampling period (80 ms). After 80 ms, the jets had essentially attained their steady-state values and we could then be confident in the constant-force approximation.

The mass properties remained constant[¶] throughout each run, and, in light of this knowledge, we set the process noise covariance to zero. For a real system with constantly fluctuating mass properties, one would normally set these covariances equal to the squares of the expected values of the deviations of the parameters over a single sampling period. We set them to zero here simply to prevent the filter gains from becoming pessimistic (too large).

The estimator was initialized by setting the states to zero and the diagonal elements of the error covariances to the squares of the true errors. One could naturally find better first estimates of the states, especially since they would be needed to generate the first jet firing command by the autopilot. The

[¶]An exception to this is that the mass was allowed to decrease in proportion to the fuel expended by the jets. As the total mass change over the simulation run was on the order of 5 slugs, the change in m^{-1} was negligible.

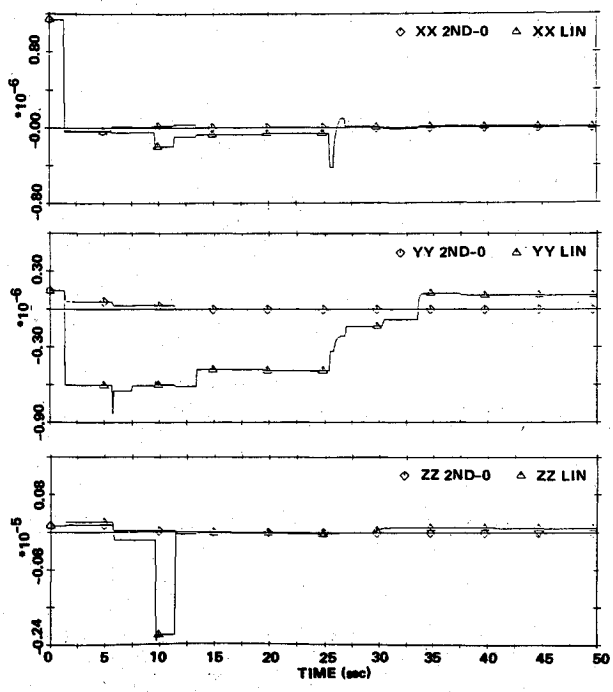

Fig. 5a Effect of second-order terms on inverse inertia estimates—diagonal elements.

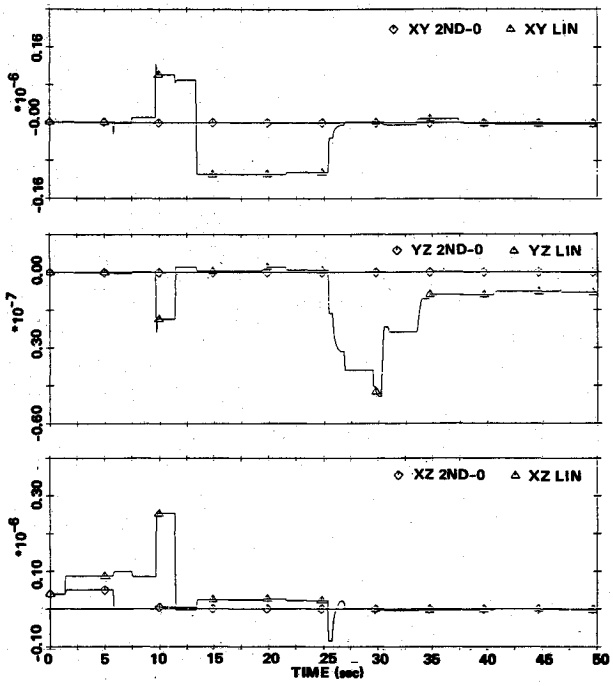

Fig. 5b Effect of second-order terms on inverse inertia elements—off-diagonal elements.

values of zero were chosen to represent a worst-case (100%) error. Whatever initial state estimates are chosen, the initial error covariance matrix should be set to the approximate level of uncertainty for best results.

Angular rate measurements were assumed to be available from a DRIRU II rate gyro package with each measurement component corrupted primarily by a quantization of 8.7×10^{-5} deg/s (1.52×10^{-6} rad/s). Linear velocity measurements from three-integrating accelerometer packages. each with component quantizations of 1.05 cm/s (0.0344 ft/s) were also assumed to be available. These accelerometers, located on the flight deck forward of the crew, are located in the vehicle frame at (90.068, −1.146, 1.833), (90.068, 0, 1.833), and (90.068, 1.146, 1.833) ft. The associated moment arm is about 58 ft.

The diagonal elements of each noise covariance matrix used in the estimator were chosen to be the variance of the density function of each measurement error component. Since the measurements used by the estimator were obtained by differencing two velocity measurements, the associated density function of the difference is a convolution. By modeling the error distribution due to the quantization q as a zero-mean uniform distribution of breadth q, the convoluted density of two such (independent) distributions is a zero-mean triangular distribution. The variance of this convolution is then $q^2/6$, or twice the variance of each of the uniform distributions. Conse-

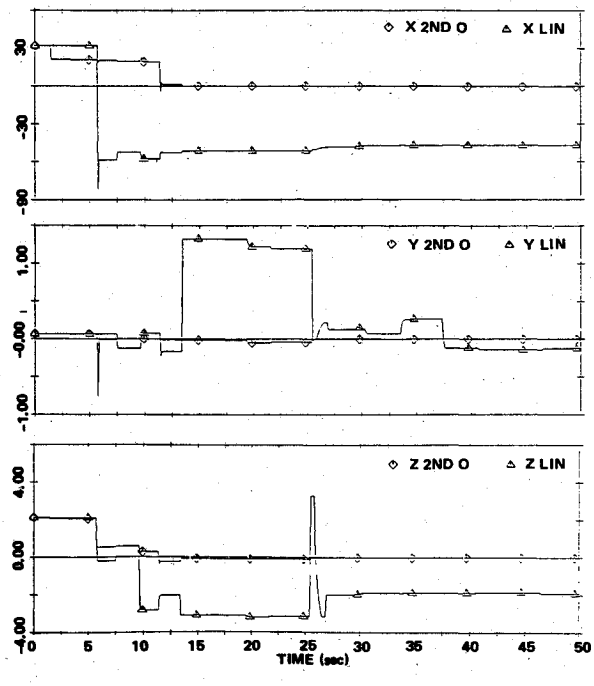

Fig. 6 Effect of second-order terms on center-of-mass location estimates.

Table 1 Mass property estimation results (50 s sample run)

Parameter	Initial estimate	Final estimate	True value	Error, %
I_{xx}^{-1}(1 slug-ft^2)	0	1.1432×10^{-6}	1.1433×10^{-6}	0.015
I_{yy}^{-1}	0	1.4819×10^{-7}	1.4818×10^{-7}	0.007
I_{zz}^{-1}	0	1.4305×10^{-7}	1.4309×10^{-7}	0.022
I_{xy}^{-1}	0	1.3723×10^{-9}	1.3781×10^{-9}	0.415
I_{yz}^{-1}	0	6.8875×10^{-11}	5.7047×10^{-11}	20.733
I_{zx}^{-1}	0	4.0035×10^{-8}	4.0055×10^{-8}	0.049
r_{cm_x} (ft)	0	3.2110×10^{1}	3.2108×10^{1}	0.005
r_{cm_y}	0	6.6617×10^{-2}	6.6667×10^{-2}	0.074
rcm_z	0	2.1333	2.1334	0.001
m^{-1}(slug^{-1})	0	1.6657×10^{-4}	1.6612×10^{-4}	1.586

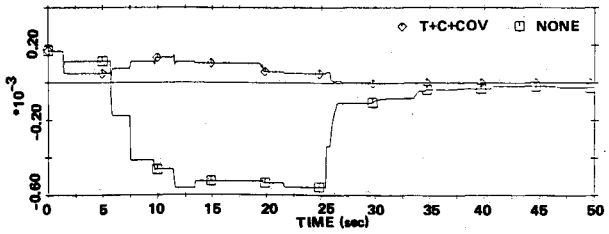

Fig. 7 Effect of rotational coupling on m^{-1} estimates.

quently, the values of the diagonal noise matrices are $(1.52\times10^{-6}$ rad/s$)^2/6$ for $\Delta\omega$ and $(0.0344$ ft/s$)^2$ for ΔV.

Mass-Property Estimation

Several maneuver histories were made to test the effects of various terms in the filter equations, with similar conclusions resulting from each scenario. For illustrative purposes we shall examine the mass property estimation for the maneuver history described in the last section whose velocity histories are given by Figs. 1 and 2. This run contains all types of maneuvers with different states being observable at different times.

Effect of Dynamic Coupling

Figures 3 and 4 illustrate the error histories of the estimates of the elements of I^{-1} and r_{cm}, respectively, for the cases where an estimate of the cross-coupling term is and is not subtracted from the measurement before processing. As is clearly seen, the coupling has a rather minor effect on the error histories, with convergence being somewhat more rapid when the coupling is subtracted off beforehand. Note that in either case the errors of the diagonal elements of I^{-1} rapidly decrease when there is a component of torque about the axis of concern. For example, the error of I_{xx}^{-1} in both cases drastically jumps from 100 to 3% after the first data incorporation. During rotation about one vehicle axis, convergence of the other diagonal elements is possible because of the small residual torque (i.e., the torque is not perfect). The estimator that subtracts out the coupling acts even better in such a situation because the subtracted term is essentailly the same size as the "signal" residual torque due to the jets.

Convergence of the off-diagonal elements of I^{-1} is slower for both cases because the parameters which are additive with respect to the diagonal elements are much less significant. Of these values, $I_{zz}^{-1}$is the most significant, and in fact its convergence is much faster than the others. The worst element of the group, $I_{yz}^{-1}$is four orders of magnitude smaller than I_{zz}^{-1}; therefore, I_{zz}^{-1}must be accurate to four digits before I_{yz} is accurate to one. Fortunately, the effect of the control system obeys the same level of significance, and I_{yz}^{-1}does not need to be known as accurately as the others.

At 25 seconds the first translation is commanded, providing the first good input for determination of the center-of-mass location is best. If only pure rotations were previously commanded, then r_{cm} would have been completely unobservable until this time and the estimation error would have been constant. Since the x and z components are more significant than the y component, these parameter estimates converged somewhat even before observability was best. After the first translation, all of the estimates of r_{cm} immediately approached the true values. Once these estimates are known well, the observability of the off-diagonal elements of I^{-1} becomes more pronounced; thus, these values also improve considerably after the first translation.

Effect of Second-Order Terms

In order to save some computation, one might wish to implement the extended (linearized) Kalman filter instead of the second-order filter. Unfortunately, such an approach does not yield acceptable estimates, as is clear in Figs. 5 and 6. The reason for the divergence is that the bias term in Equation (19) is significant when the resultant applied force is large. Previously, we observed that there is a small but noticeable residual force even during rotational maneuvers. This small force is significant enough to cause the filter to diverge.

Figure 7 illustrates the effects of including estimates of the transverse and centripetal accelerations during the estimation of m^{-1}. Since the angular rates are predominantly small, no difference whatsoever can be observed by excluding the centripetal acceleration from the measurement. Even the consistency functions appear identical. The effect of the transverse acceleration is more significant, however, and excluding it altogether causes the estimation error to diverge until a large translational maneuver with little rotation is commanded. Even after this point, the residuals remain inconsistent and the final error is large (15% vs 1% of the initial error).

Table 1 summarizes the final estimation error obtained at the end of the sample 50-s run. This table assumes that transverse accelerations (with residual covariance incrementation) and dynamic coupling effects are estimated and subtracted out, and that the second-order filter is used to estimate I^{-1} and r_{cm}. The estimation error for the mass reciprocal actually increased slightly during the final rotational maneuvers; its best value was 0.231% during the translational maneuvers.

A significant improvement in performance also results by adding into the residual covariance the covariance of the uncertainty of the estimate of the transverse acceleration. Neglecting this uncertainty, which is often as large as the measurement noise, results in larger estimation errors, especially when the net translations are small. Moreover, the final error is about three times as large as that of the filter that includes the term. Therefore, the best performance is achieved by subtracting the transverse acceleration and increasing the residual covariance accordingly, at least for this particular system.

Conclusion

The results of this research establish that the on-line identification of the inverse inertia matrix, the center-of-mass location, and the mass reciprocal for a spacecraft is feasible once the equations of motion are formulated in terms of a nonlinear state estimation problem. By filtering noisy measurements of the spacecraft's angular and linear velocities and by assuming that the unmodeled disturbance forces and torques are small and essentially random, estimates of the mass-property parameters can be generated that track the true values. Furthermore, the residuals associated with the resulting filter can be used to identify mass-property jumps.

Acknowledgment

This work was performed at The Charles Stark Draper Laboratory, Inc. under Independent Research and Development. The authors gratefully acknowledge this support.

References

[1]Bergmann, E.V., et al., "An Advanced Spacecraft Autopilot Concept," *Journal of Guidance and Control,* Vol. II, No. 3, May-June 1979, p. 161.

[2]Crawford, B.S., "Operation and Design of Multi-jet Spacecraft Control System," C.S. Draper Laboratory, Cambridge, MA, T-509 Sept. 1968.

[3]Gelb, A., et al., *Applied Optimal Estimation,* M.I.T. Press, Cambridge, MA, 1974.

[4]Brun, H., "Development and Analysis of Non-Linear Mass Property Estimator," C.S. Draper Laboratory, Cambridge, MA., T-885 June 1985.

[5]Denham, W.F. and S. Pines, "Sequential Estimation When Measurement Function Nonlinearity Is Comparable to Measurement Error," *AIAA Journal*, Vol. 4, No. 6, June 1966, pp. 1071-1076.

[6]Chow, E.Y., "Analytical Studies of the Generalized Likelihood Ratio Technique for Failure Detection," M.S. Thesis, Dept. of Electrical Engineering and Computer Science, M.I.T, Cambridge, MA, Jan. 1976.

[7]Levy, D.R., "Mass Property Estimation with Jet Failure Identification for Control of Asymmetrical Satellites," C.S. Draper Laboratory Cambridge, MA, T-831, Dec. 1983.

[8]Jazwinski, A.H., *Stochastic Processes and Filtering Theory*, Academic Press, New York, 1970.

[9]Richfield, R.F., "Input Selection and Convergence Testing for Use with a Second Order Mass Property Estimator," C.S. Draper Laboratory, Cambridge, MA, CSDL-T-884, June 1985.